Supporting Information

Song et al. 10.1073/pnas.1317026110

SI Materials and Methods

Induction of Genetic Events. The 4-OH-tamoxifen (4OHT; Sigma) was dissolved in 90:10 sunflower oil/ethanol by ultrasound sonication for 10 min to a final concentration of 10 mg/mL. To induce genetic events, adult mice (mean 3.5 ± 0.6 mo) were injected intraperitoneally with 1 mg per mouse per day for 5 consecutive days with freshly prepared 4OHT.

Recombined Allele Detection by PCR. DNA was obtained from 4OHT-induced cortex (~2 mm^3 tissue) of *TR* mice using solution A [25 mM NaOH/0.2mM EDTA (100 μL) at 95 °C for 1 h]. Upon adding solution B [40 mM Tris·HCl (100 μL)], samples were vortexed briefly and centrifuged for 10 min at 376 × *g*. One microliter of supernatant was used in 25 μL of total PCR. Germline genotyping was performed as previously described (1–3). The expected products are as follows: T_{121} = ~300 bp; *KRAS*: wt = 622 bp, LSL-cassette = 500 bp, and recombined = 650 bp.

In Situ RNA Hybridization. In situ RNA hybridization was performed on paraffin sections using ^{35}S-UTP labeled riboprobes as described (4). The plasmid (gifted by Dr. Peter, Duke University, Durham, NC) containing murine VEGF-A165 cDNA was linearized with XbaI to generate antisense probes to detect all VEGF-A transcripts, and by BamHI to generate sense probes as a negative control. Sections were viewed under bright and dark field.

Histopathology and Immunohistochemistry. Haematoxylin/eosin (H&E) staining was performed on formalin-fixed and paraffin-embedded sections as described previously (1, 2). Details of histopathological evaluation are given below. Immunohistochemistry (IHC) was performed as described previously (1, 2) (see Table S6 for primary antibodies information).

Histopathological Evaluation. H&E-stained, sagittal sections of the entire brain from all available mice were evaluated by C.R.M. and D.N.L., and tumors were graded based upon the current World Health Organization (WHO) classification for human astrocytomas (5, 6). GFAP, S100β protein, synaptophysin, CD31, and CD45 immunostained sections were also evaluated as required for accurate diagnosis. Because the current models use systemically administered 4OHT to induce genetic events, diffuse activation of transgene expression was evident (Fig. S2*B*), and widespread astrocyte proliferation was expected. For this reason, the distinction between early—focal astrocyte proliferation in mice receiving 4OHT with diagnosis as diffuse astrocytoma (WHO grade II, A2)—and normal astrocytes with diagnosis as "normal brain" was difficult in certain cases. Therefore, the following criteria were adopted. Tumors were designated A2 if cytologically atypical astrocytes and more than one of the following secondary structures of Scherer were evident: subpial condensation, perineuronal satellitosis, and perivascular satellitosis. Evidence of increased mitotic activity (more than an occasional mitotic figure in the examined H&E-stained section) was required for a diagnosis of anaplastic astrocytoma (WHO grade III, AA). Glioblastomas (GBM) were evident only in *TR*, $TRP^{L/+}$, and $TRP^{L/L}$ mice, and such tumors universally contained necrosis, either geographic or pseudopalisading. Dilated vasculature and intravascular thrombosis was invariably evident as well, but neither endothelial proliferation, as evidenced by multilayering, nor microvascular proliferation was identified. All astrocytomas were evident as diffuse astrocytic proliferation with variable anatomic localization that included the neocortex, diencephalon, brainstem, spinal cord, and olfactory bulb.

Apoptosis and Proliferation Assays. Apoptosis by TUNEL assay and proliferation by Ki67 IHC were as previously described (7). Apoptosis and proliferation indices were enumerated on adjacent immunostained sections in mice killed at 2 mo post induction (p.i.) and quantified with ImageJ (http://rsbweb.nih.gov/ij/) using images taken from five random fields in the same area of the brain.

Stereotaxic Injection. Stereotaxic injection was as described previously (8). In brief, mice were anesthetized with avertin and placed into a stereotaxic frame (David KOPF Instruments). One microliter of self-deleting recombinant lentivirus PTK-627 (~10^9 particles per ml) was delivered with an infusion pump (Sage Laboratory, Orion Research) at a rate of 0.1 μL/min. Coordinates used were as follows: (A, L, D) = 0, 1, and 1.2 mm from the Bregma suture. These coordinates target the frontal cerebral cortex.

MR Imaging and 3D Vascular Reconstruction. T1 pre- and post-Gadolinium enhanced magnetic resonance images (MRI) and T_2-weighted images were acquired as described previously (9) at 14 wk p.i. for $TRP^{L/+}$ mice, with follow up MRI performed at 2-wk intervals. Tumor volumes were calculated using ImageJ software. Regions of interest (ROI) were drawn slice by slice on the whole tumors using T_2-weighted images, which demonstrated good contrast between tumor and healthy brain tissue. Volumes were calculated as a product of the total ROI area multiplied by the slice thickness (0.5 mm). For some tumors, magnetic resonance angiographic (MRA) images were also acquired, and vessels were extracted and analyzed for vessel number, radius, and tortuosity in the tumor vicinity, as described (9).

qPCR Detection of PTEN Loss. Tissues were scraped from nonstained paraffin-embedded tissue sections, and DNA was extracted as previously described (10). H&E-stained serial sections were used to locate tumor masses. Customized *PTEN* TaqMan assays (Applied Biosystems of Life Technologies; 186220104_PTEN) and standard PCR cycling conditions were used. Tail DNA, cultured $TRP^{L/L}$ cells, and $TRP^{L/L}$ tumors were used as controls. $\Delta\Delta C_t$ = (sample C_t[*PTEN*] − sample C_t[*β-actin*]) − ($PTEN^{+/+}$ control Ct[*PTEN*] − $PTEN^{+/+}$ control C_t[*β-actin*]). C_t = the number of cycles required to reach a threshold value, which is set within the exponential phase of the logarithmic scale amplification plot. Analysis of control samples indicates copy numbers of 2, 1, and 0 by $2^{-\Delta\Delta Ct}$ values of >0.6, 0.15–0.6, and <0.15, respectively.

Statistical Analysis. Student *t* test was performed for mean comparisons of continuous variables. All statistical tests were two-sided, and $P < 0.05$ was considered significant unless otherwise stated. Kaplan–Meier survival curves were plotted using GraphPad Prism 5, and log-rank test analysis was used for comparisons of median overall survival (OS).

1. Xiao A, Wu H, Pandolfi PP, Louis DN, Van Dyke T (2002) Astrocyte inactivation of the pRb pathway predisposes mice to malignant astrocytoma development that is accelerated by PTEN mutation. *Cancer Cell* 1(2):157–168.

2. Xiao A, et al. (2005) Somatic induction of Pten loss in a preclinical astrocytoma model reveals major roles in disease progression and avenues for target discovery and validation. *Cancer Res* 65(12):5172–5180.

3. Jackson EL, et al. (2001) Analysis of lung tumor initiation and progression using conditional expression of oncogenic K-ras. *Genes Dev* 15(24):3243–3248.
4. Yin C, Knudson CM, Korsmeyer SJ, Van Dyke T (1997) Bax suppresses tumorigenesis and stimulates apoptosis in vivo. *Nature* 385(6617):637–640.
5. Raza SM, et al. (2004) Identification of necrosis-associated genes in glioblastoma by cDNA microarray analysis. *Clin Cancer Res* 10(1 Pt 1):212–221.
6. Raza SM, et al. (2002) Necrosis and glioblastoma: A friend or a foe? A review and a hypothesis. *Neurosurgery* 51(1):2–12, discussion 12–13.
7. Hill R, Song Y, Cardiff RD, Van Dyke T (2005) Heterogeneous tumor evolution initiated by loss of pRb function in a preclinical prostate cancer model. *Cancer Res* 65(22): 10243–10254.
8. Doetsch F, Caillé I, Lim DA, García-Verdugo JM, Alvarez-Buylla A (1999) Subventricular zone astrocytes are neural stem cells in the adult mammalian brain. *Cell* 97(6): 703–716.
9. Bullitt E, et al. (2006) Malignancy-associated vessel tortuosity: A computer-assisted, MR angiographic study of choroid plexus carcinoma in genetically engineered mice. *AJNR Am J Neuroradiol* 27(3):612–619.
10. Hill R, Song Y, Cardiff RD, Van Dyke T (2005) Selective evolution of stromal mesenchyme with p53 loss in response to epithelial tumorigenesis. *Cell* 123(6): 1001–1011.

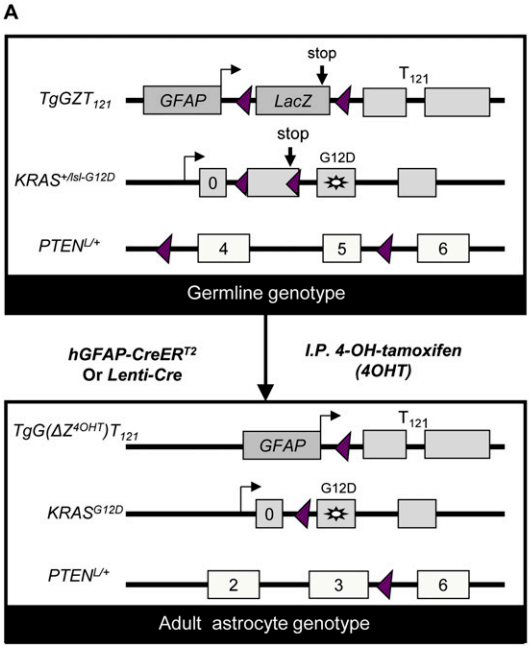

B Genotype abbreviations.

Abbr	Genotype (after 4-OHT)
C	*Control*
T	$TgG(\Delta Z^{4OHT})T_{121}$
R	$KRAS^{G12D}$
$P^{L/+}$	$PTEN^{L/+}$
$P^{L/L}$	$PTEN^{L/L}$
$RP^{L/+}$	$KRAS^{G12D}$;$PTEN^{L/+}$
$RP^{L/L}$	$KRAS^{G12D}$;$PTEN^{L/L}$
$TP^{L/+}$	$TgG(\Delta Z^{4OHT})T_{121}$;$PTEN^{L/+}$
$TP^{L/L}$	$TgG(\Delta Z^{4OHT})T_{121}$;$PTEN^{L/L}$
TR mock	$TgGZT_{121}$;$KRAS^{+/lsl\text{-}G12D}$ (wild-type)
TR	$TgG(\Delta Z^{4OHT})T_{121}$;$KRAS^{G12D}$
$TRP^{L/+}$	$TgG(\Delta Z^{4OHT})T_{121}$;$KRAS^{G12D}$;$PTEN^{L/+}$
$TRP^{L/L}$	$TgG(\Delta Z^{4OHT})T_{121}$;$KRAS^{G12D}$;$PTEN^{L/L}$

Except C (control), all the other genotypes include *hGFAP-CreER*$^{T2+/-}$. Controls were mice with wildtype T, R, or P alleles but *hGFAP-CreER*$^{T2+/-}$ or *hGFAP-CreER*^{T2} negative animals.

Fig. S1. Genotypes of inducible astrocytoma GEM models. (*A*) $TgGZT_{121}$ with human *GFAP* promoter-driven floxed LacZ stop cassette and downstream T_{121} gene (1); $KRAS^{+/lsl\text{-}G12D}$, a knock-in with a constitutively active mutated $KRAS^{G12D}$ and an upstream floxed stop cassette; and $PTEN^{L/+}$, a single Cre-conditional null allele with floxed exons 4 and 5. $PTEN^{L/L}$ mice homozygous for the conditional null allele were also assessed. At 3 mo of age, mice were either crossed to *hGFAP-CreER*^{T2} mice to generate *T*, *R*, and $P^{L/+}$ mice after systemic administration (IP) of 4OHT, or injected intracranelly with self-deleting Cre-lentivirus to induce genetic events. ◄, LoxP sites; ↓, transcriptional stop signals. (*B*) Abbreviations for all single-, double-, and triple-transgenic GEM mice also harboring an *hGFAP-CreER*^{T2} allele are listed.

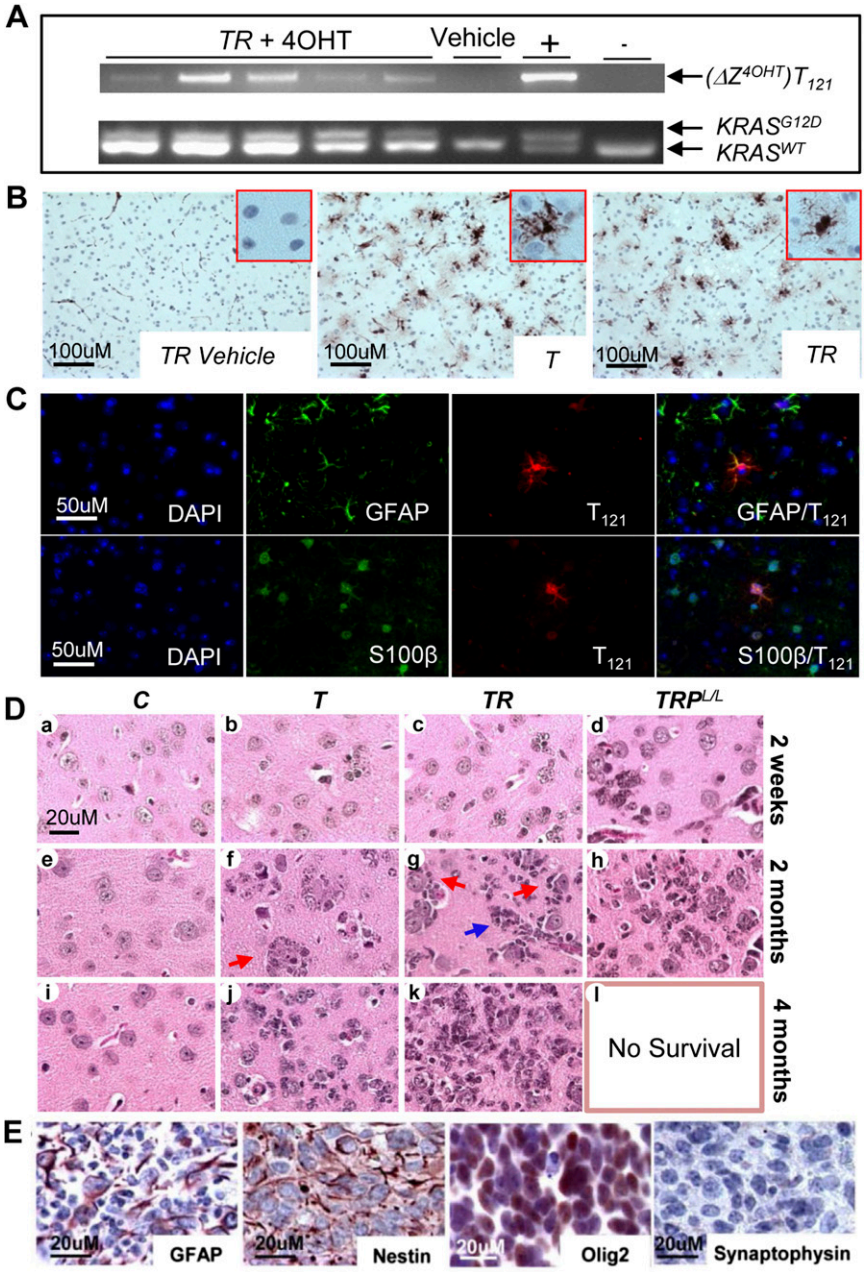

Fig. S2. Induction of oncogenic events in adult GEM astrocytes and temporal pattern of astrocytoma development. (*A*) PCR analyses of five paraffin-embedded *TR* brains harvested at 2 mo p.i. demonstrate the presence of $(\Delta Z^{4OHT})T_{121}$, $KRAS^{G12D}$, and wild-type *KRAS* alleles. The wild-type *KRAS* allele product, and no recombination-specific product are present in vehicle-treated *TR* mice. Positive controls were from $Tg(\Delta Z)T_{121}$ and $KRAS^{+/lsl\text{-}G12D}$;*GFAP-Cre* mice, respectively. A wild-type BDF1 mouse served as a negative control. (*B*) Immunohistochemistry analysis showed that T_{121} expression in *T* and *TR*, but not in *TR* vehicle treated brains 2 wk p.i.. Insets show high magnification images of immunoreactive cells. (*C*) Astrocyte-specific expression of T_{121} in *TR* mice 2 wk p.i. was confirmed by immunofluorescence staining. T_{121} expression (red) colocalized with that of both GFAP (green, *Upper*) and S100β (green, *Lower*). DAPI was used to counterstain nuclei. (*D*) H&E-stained sections of littermate control (C), *T*, *TR*, and $TRP^{L/L}$ mice at 2 wk, 2 mo, and 4 mo p.i.. Representative cortical high cell density regions (other than tumor masses, if present) were imaged for each time point and mutant. Mutants frequently showed diffuse proliferation of atypical astrocytes with formation of perineuronal (*f* and *g*, red arrows) and perivascular satellites (*g*, blue arrow) compared with similarly treated control brains (*a*, *e*, and *i*). Cortical hypercellularity was evident after 2 wk, 2 mo, and 4 mo p.i. in *T* (*b*, *f*, and *j*), *TR* (*c*, *g*, and *k*), and $TRP^{L/L}$ (*d* and *h*) mice, respectively. $TRP^{L/L}$ mice did not survive beyond 4 mo p.i.. (*E*) Immunostaining of GFAP, nestin, olig2, and synaptophysin in $TRP^{L/L}$ GBM.

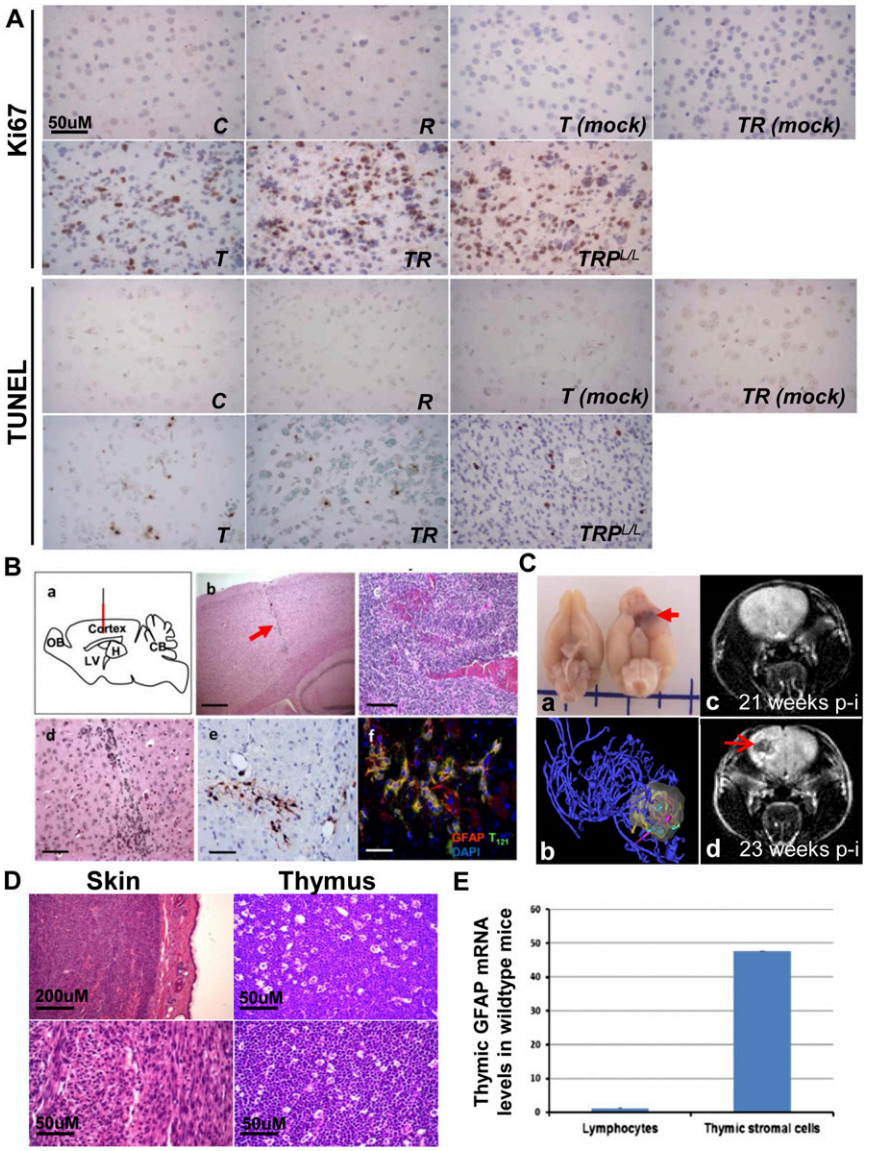

Fig. S3. (*A*) Representative images of Ki67 and TUNEL staining in 2 wk post 4OHT or mock injected brain of indicated genotypes. (*B*) Stereotaxic injection of self-deleting-*Cre* lentivirus into frontal cortex to assess focally induced pathology. (*a*) Schematic diagram illustrates the injection procedure. OB, olfactory bulb; CB, cerebellum; LV, lateral ventricle; H, hippocampus. (*b*) H&E-stained section of injected brain with needle track (arrow). (*c*) H&E-stained section of GEM-GBM arising in injected $TRP^{L/+}$ mouse. (*d*) H&E-stained serial section of region surrounding the needle track (2 wk post virus injection shows an aberrant cell population that is positive for T_{121} expression based on IHC (*e*) and stains for both T_{121} (green) and GFAP (red) by immunofluorescence staining (*f*). (Scale bars: 800 μm (*b*) and 50 μm (*c*–*e*). (*C*, *a*) Brain with gross tumor mass (red arrow). (*b*) Magnetic resonance angiographic (MRA) images-obtained 3D computer-enhanced vascular reconstruction showed vessel tortuosity both extrinsic (blue) and intrinsic (red, gold, yellow, and cyan lines) to the tumor mass. (*c* and *d*) Representative magnetic resonance images (MRI) showing a $TRP^{L/+}$ mouse imaged at 21 and 23 wk p.i.. A tumor (red arrow, *d*) developed within a 2-wk interval subsequent to a normal scan (*c*). Eleven animals were serially imaged, and tumor volume was quantified in Fig. 4*A*. (*D*) Representative H&E-stained images of skin and thymic lesions that sometimes presented before full brain disease development. Skin lesions were frequent in $RP^{L/L}$ mice, which developed no brain pathology. Thymus was often significantly enlarged with expansion of both cortical and medullar regions. (*E*) GFAP mRNA levels in thymic lymphocytes and stromal cells of wild-type mice by RT-qPCR.

Table S1. PCR primers and cycling conditions for detecting *LoxP* site recombination

Allele	Primers	Cycles	Conditions
$TgGZT_{121}$	5′ TGA TCA GAA CCA TCA TG 3′	35	94 °C for 5 min
	5′ GTT GAC CAG AGT GGC GTA GG 3′		94 °C for 1 min
			55 °C for 1 min
			72 °C for 5 min
$KRAS^{+/lsl\text{-}G12D}$	5′ GTC TTT CCC CAG CAC AGT GC 3′	34	95 °C for 2 min
	5′ CTC TTG CCT ACG CCA CCA GCT C 3′		95 °C for 30 s
	5′ AGC TAG CCA CCA TGG CTT GAG TAA GTC TGC A 3′		61 °C for 30 s
			72 °C for 45 s
			72 °C for 10 min

Table S2. Phenotype summary in mice with brain tumors or other phenotypes as COD

	Brain tumor as COD								
Genotype	A2	AA	GBM	HGA	HGA, %	Total	Other lesions as COD	Censored	Total
*T**	0	0	0	0	0	0	0	11	11
R†	0	0	0	0	0	0	2(SL), 3(TL)	6	11
$RP^{L/+}$†	0	0	0	0	0	0	2(SL), 1(TL)	4	7
$RP^{L/L}$†	0	0	0	0	0	0	11(SL)	3	14
$TP^{L/+}$*	0	0	0	0	0	0	1(SL), 1(TL)	6	8
$TP^{L/L}$*	0	0	0	0	0	0	2(SL)	9	11
TR	0	10	3	13	100	13	1(TL)	7	21
$TRP^{L/+}$	0	8	12	20	100	20	6(SL), 2(TL)	0	28
$TRP^{L/L}$	0	1	7	8	100	8	5(SL)	4	17
Total	0	19	22	41	100	41	37	50	128

A2, grade II astrocytoma; AA, anaplastic astrocytoma; COD, cause of death; GBM, glioblastoma multiforme; HGA, high-grade astrocytoma; SL, skin lesions; TL, thymic lesions.

*Nine of 11 *T* animals developed grade II astrocytoma by 15 mo of age, but did not die from the desease. $TP^{L/+}$ and $TP^{L/L}$ animals also developed grade II astrocytoma but did not cause the death.

†*R, $RP^{L/+}$, and $RP^{L/L}$* animals did not develop any brain pathology.

Table S3. Loss of *PTEN* alleles in *TR* and $TRP^{L/+}$ tumors by qPCR

Mouse ID	Genotype	DNA source	$2^{-\Delta\Delta Ct}$	No. of *PTEN* allele
1	$PTEN^{+/+}$ (G)	Tail DNA	1	2
2	$PTEN^{+/-}$ (G)	Tail DNA	0.48	1
3	$PTEN^{L/L}$ (S)	Cultured cells	0.02	0
4	$TRP^{L/L}$ (S)	Tumor mass	0.05	0
5	$TRP^{L/L}$ (S)	Tumor mass	<0.01	0
6	$TRP^{L/L}$ (S)	Tumor mass	<0.01	0
7	$TRP^{L/L}$ (S)	Tumor mass	<0.01	0
8	$TRP^{L/+}$ (S)	Necrosis center	<0.01	0
8	$TRP^{L/+}$ (S)	Tumor mass	<0.01	0
9	$TRP^{L/+}$ (S)	Necrosis center	0.56	1
10	$TRP^{L/+}$ (S)	Tumor mass	1.7	2
11	$TRP^{L/+}$ (S)	Tumor mass	<0.01	0
12	$TRP^{L/+}$ (S)	Necrosis center	0.09	0
12	$TRP^{L/+}$ (S)	Tumor mass	0.04	0
13	$TRP^{L/+}$ (S)	Tumor mass	0.91	2
13	$TRP^{L/+}$ (S)	Necrosis center	0.05	0
14	$TRP^{L/+}$ (S)	Tumor mass	1.14	2
15	$TRP^{L/+}$ (S)	Tumor mass	1.66	2
16	$TRP^{L/+}$ (S)	Tumor mass	0.13	0
17	*TR*	Tumor mass	0.298	1
17	*TR*	Tumor mass	<0.01	0
18	*TR*	Tumor mass	0.34	1
19	*TR*	Tumor mass	0.43	1
19	*TR*	Necrosis center	<0.01	0
20	*TR*	Tumor mass	0.97	2
21	*TR*	Tumor mass	0.49	1
22	*TR*	Tumor mass	0.49	1

Analysis of control samples indicates copy numbers of 2, 1, and 0 by $2^{-\Delta\Delta Ct}$ values of >0.6, between 0.15–0.6, and <0.15, respectively. Loss of a single and both copies of *PTEN* was statistically significant by Binomial exact test ($P < 0.01$) assuming a random probability of 1%. G, germ-line deletion; S, somatic deletion (conditional knockout) of *PTEN*.

Table S4. *Trp53* status by sequencing and p53 protein localization by IHC in HGAs

Tumor ID	Genotype	DNA source	Diagnosis	*Trp53* status (corresponding human mutation)	p53 localization
1	*T*	ctx	A2	WT	Negative
2	*T*	ctx	A2	WT	Negative
3	*T*	ctx	A2	WT	Negative
4	*TR*	Tumor mass	GBM	WT	Cyto
5	*TR*	Tumor mass	GBM	WT*	Cyto/Nuc[†]
6	*TR*	Tumor mass	GBM	WT[‡]	Nuc
7	*TR*	Tumor mass	GBM	A135V (A138V)	Nuc
8	TR	Tumor mass	AA	WT	Cyto
9	TR	Tumor mass	AA	WT	Cyto
10	TR	Tumor mass	AA	K318 frame shift[§]	Nuc
11	TR	Tumor mass	AA	M234I (M237I)	Nuc
12	$TRP^{L/+}$	Tumor mass	GBM	WT[‡]	Nuc
13	$TRP^{L/+}$	Tumor mass	GBM	WT	Cyto
14	$TRP^{L/+}$	Tumor mass	GBM	A135V (A138V)	Nuc
15	$TRP^{L/+}$	Tumor mass	GBM	V170L (V173L)	Nuc
16	$TRP^{L/+}$	Tumor mass	GBM	R279H	Nuc
17	$TRP^{L/+}$	Tumor mass	AA	R155 in frame insertion[§]	Nuc
18	$TRP^{L/+}$	Tumor mass	AA	WT[‡]	Negative
19	$TRP^{L/L}$	Tumor mass	GBM	WT	Cyto
20	$TRP^{L/L}$	Tumor mass	GBM	WT	Cyto
21	$TRP^{L/L}$	Tumor mass	GBM	R153P (R156P)	Nuc
22	$TRP^{L/L}$	Tumor mass	GBM	V170M (V173M)	Nuc
23	*T*	Primary cells derived from ctx	A2	WT	Negative
24	*T*	Primary cells derived from ctx	A2	WT	Negative
25	*T*	Primary cells derived from ctx	A2	WT	Negative
26	*TR*	Primary cells derived from tumor mass	GBM	V170M (V173M)	Nuc
27	*TR*	Primary cells derived from tumor mass	GBM	S212R (S215R)	Nuc
28	*TR*	Primary cells derived from tumor mass	GBM	V213M (V216M)	Nuc
29	*TR*	Primary cells derived from tumor mass	GBM	R279H	Nuc
30	*TR*	Primary cells derived from tumor mass	GBM	K316 frame shift[§]	Nuc
31	*TR*	Primary cells derived from ctx	AA	V213M (V216M)	Nuc
32	*TR*	Primary cells derived from ctx	AA	R155P (R158P)	Nuc
33	*TR*	Primary cells derived from ctx	A2	WT	Negative

Genomic DNA was prepared from either HGA tumor tissues, except T animals [cortex tissues (ctx) because they did not develop HGAs], or primary cells derived from tumor masses or ctx. Parentheses indicate corresponding human *TP53* missense mutations detected in human GBMs (http://p53.iarc.fr/; IARC *TP53* database R16). p53 protein localization was assessed by immunostaining. Nuc, nucleus; Cyto, cytoplasm. Additional five grade III tumors sequenced had no coding region mutations, which may be due to frozen tissues used for sequencing not matched with tissues used for histological evaluation because some grade III tumors had no obvious gross mass.

*Splice site acceptor was mutated at −1 position on exon 5.

[†]Two masses were developed in this mouse brain (one with cytoplasmic p53 and the other one with nuclear p53). It is not known which mass was used for sequencing.

[‡]Mutations had been found in intronic regions without known SNP.

[§]Corresponding human *TP53* frame shifts were also found in human GBMs.

Table S5. p53 protein detected by IHC at different time points p.i.

Genotype (time p.i.*)	Tissue type (pathology)†	Total no.‡	No. negative	No. with any p53 positivity	Staining pattern§	p53 positivity, % of mice
R (3–6 mo)	Brain (normal)	3	3	0	NA	0
T (<5 mo)	Brain (A2)	8	8	0	NA	0
T (12–18 mo)	Brain (A2)	14	9	5	Clusters; >20 cells +	36
TP^L (7–12 mo)	Brain (A2)	4	4	0	NA	0
TR (2 wk)	Brain (A2)	6	6	0	NA	0
TR (2 mo)	Brain (A2)	9	8	1	Single cluster; cyto	11
TR (3 mo)	Cortex/ob (A2)	5	2	3	Nodules nuc/cyto	60
TR (3 mo)	Cortex/ob (AA)	1	0	1	Mass Nuc	100
TR (4 mo)	Cortex/ob (A2)	4	0	4	Nodules nuc/cyto	100
TR (4 mo)	Cortex/ob (AA)	5	0	5	Mass nuc/cyto	100
TR	Tumor (GBM)	7	0	7	Mass nuc/cyto	100
TRP^L (2–4 mo)	Tumor (AA)	9	0	9	Mass nuc/cyto	100
TRP^L	Tumor (GBM)	18	0	18	Mass nuc/cyto	100

*Time post induction (p.i.) of engineered events, with induction occurring at 3 mo of age.
†A2, grade II; AA, grade III; GBM, glioblastoma (grade IV); ob, olfactory bulb.
‡Each sample was from independent mouse.
§Robust nuclear (nuc) or cytoplasmic (cyto) p53 staining in clusters, nodules, or tumor masses.

Table S6. Antibodies used in immunostaining

Antibody	Clone/cat. no.	Dilution	Supplier
T_{121} mouse monoclonal	N-terminal–specific Ab2	1:300 IHC; 1:100 IF	Calbiochem
Ki67	M-19	1:1,500	Santa Cruz
GFAP	Z0334	1:500	DAKO
Olig2	sc-19969	1:200	Santa Cruz
Synaptophysin	A0010	1:50	DAKO
Nestin	NB100-1604	1:10,000	Novus
S100β	Ab52642	1:400	Abcam
p53	NCL-p53-CM5P	1:500	Novocastra

IHC, immunohistochemistry; IF, double immunofluorescence staining.